Palm-sized quadrotor source localization using modified bio-inspired algorithm in obstacle region

Muhamad Rausyan Fikri[1], Djati Wibowo Djamari[2]
[1]Department of Information Systems, Sampoerna University, Jakarta, Indonesia
[2]Department of Mechanical Engineering, Sampoerna University, Jakarta, Indonesia

Article Info

ABSTRACT

This paper uses a palm-sized quadrotor to demonstrate the gas source localization (GSL) in obstacle regions. The chemical substance performs a dilute dispersion in the air, and it is challenging to locate the source position. The difficulty level of the GSL increases if the location is in the obstacle region. To estimate the gas source position, it indeed uses high computational cost systems. However, it leads to a new problem: a palm-sized quadrotor has a limited size and payload capacity. In this paper, a search based on the silkworm moth is employed. The algorithm works straightforwardly as the detection gas triggers its motion. A repulsion function is integrated into a searching method to compensate the algorithm for working in single surface obstacle regions. The validation data and the palm-sized quadrotor design are provided to convince the search effectiveness performance.

Corresponding Author:

Muhamad Rausyan Fikri
Department of Information Systems, Sampoerna University
Jakarta, Indonesia
Email: muhamad.fikri@sampoernauniversity.ac.id

1. INTRODUCTION

This paper is an extended work on gas source localization (GSL) [1]. In a study [1], the validation of GSL performance was conducted in an open-space environment. The robot's ability to discover the gas source is an attractive topic with various proposed methods [2]–[5]. Implementing the GSL is a challenging engineering problem due to the frequently diluted gas distribution. On the other hand, the performance of the GSL is helpful for some applications such as finding victims in a disaster area and locating the source of gas leakage in mining companies [6]–[9], forest fires [10], [11] and investigating fruit maturity [12], [13]. A comprehensive study of the GSL is available in [14]. The implementation of GSL shows some promising features; however, estimating the source position from the gas characteristics is challenging thanks to its complexity and turbulent distribution [15]. When it contacts the air [16], the challenge may increase significantly with a particular assumption that this task is performed in a disaster area with obstacles surrounding the system's range of interest (RoI).

In the previous study, some methods for GSL from animal behavior, known as the term reactive searching, have been proposed. This technique is inspired by animal behavior, such as drosophila [17], the navigation strategies of mice [18], bio-inspired Levy Taxis [19], bat algorithm [20], and mating partner seeking behavior by the moth [1], [2], [21]–[23]. To name of few, 3D investigation is also conducted by [2], [5], [19], [24], [25]. However, the research focuses on the open space area, and few use quadrotors. On the other hand, some methods have already been proposed from non-animal behavior or active searching. In the study [3], a particle filter algorithm is employed to locate the gas in a quadrotor. Hutchinson *et al.* [26]

employ an information-theoretic method to perform source localization, and [5] employ a fuzzy-based filter. The implementation requires high computational resources and impacts the palm-sized quadrotor's payload. The integration of GSL and vision systems using a camera is also reported in some works [27], [28], where it is said to implement the search using vision systems increases the payload significantly and reduces its agility. Vision implementation is limited to specific applications such as mapping and perceiving the source [29]–[32]. The drawbacks are the time duration needed to inspect the environment entirely for mapping and the strong object assumption for the vision-based source localization. On the other hand, the GSL in an unknown environment often encounters obstacles. In this situation, the palm-sized quadrotor with the efficient payload could be the option because it can maneuver freely, is agile, and has less computational cost, especially when the system integrates with the obstacle avoidance techniques. Then, developing the technique for searching while avoiding obstacle is essential. According to the previous works [1] and [33], using silkmoth behavior shows a promising result in searching performance. In this work, Russell *et al.* [34] and Kowadlo and Russell [35] also noted that the silkmoth exhibits a direct action when receiving the female moth's pheromone.

Knowing the potential of searching and obstacle avoidance techniques can be implemented in this situation. Thus, this study proposes two contributions. The first is developing more efficient sensing systems than the previous [1]. Some modification is introduced to support the palm-sized quadrotor performing GSL in a confined area. The second contribution is developing a collaborative algorithm between the GSL and the obstacle avoidance algorithm. Here, the sensor position is a priority to conduct the investigation. An experimental validation using particle image velocimetry (PIV) is introduced. The avoidance algorithm is based on the repulsion force artificially sensed by the distance sensors. Therefore, the mathematical method of this idea is elucidated in this paper.

The content of this paper is organized as follows: In section 2 focuses on the problem statements to have a clear goal of this research direction. The explanation of the silkmoth behavior mechanism of the GSL, data processing technique, and obstacle avoidance will be elucidated in section 3. In section 4, the evaluation of sensor position is performed using PIV. The description of the experimental design to evaluate the quadrotor performance in an obstacle region will be delivered in section 5. Finally, the discussion and conclusion of our study will be given in sections 6 and 7.

2.   THE PROPOSED METHOD

In this section, three components fof the palm-sized quadrotor are discussed. The first is the command execution system (CES) design for GSL and obstacle avoidance, the second is GSL system workflow, and the third is sensors selection and layout. The dynamics and searching mechanism and the experimental design for searching validation are also discussed. The problem in this paper is formally introduced in the problem statement.

2.1. Problem statements

A small take-off weight capacity causes a significant payload constraint in a palm-sized quadrotor. Consequently, the energy resource is minimal, and the sensing system size and weight are minimal. In this case, the flight duration is short. Additionally, a palm-sized quadrotor must carry the other systems, such as a distance sensor for obstacle avoidance. Here, two main issues are considered to search in the obstacle region: A palm-sized quadrotor component design for gas localization and avoiding obstacles. In this case, the proper selection for the system can be decided carefully. Second, determining the method to maintain the searching in the obstacle region under the time constraint. Here, the modified bioinspired algorithm is introduced.

The palm-sized quadrotor uses parrot mini-drone mambo FPV (Parrot Inc), where flight duration information in a palm-sized quadrotor without payload is 10 minutes. The flight duration becomes significantly shorter as the payload increases, around 5 to 8 minutes. Then, determining the quadrotor dimension was discussed in [1], [23], [36], where the dimension of a palm-sized quadrotor was approximately 130 mm. The reference for payload limitation is based on [1], with the maximum payload is must less than 40 g.

The next step is to embed the modified bioinspired algorithm into the system. The modified bioinspired algorithm consists of searching based on silkmoth behavior and potential function. The algorithm's effectiveness will be validated through experimental trials. First, however, a brief description is included to explain how the palm-sized quadrotor can maneuver in the obstacle region. The environment for the searching method validation uses two designs. The first design is a blocked space where the obstacle placed in the front of the gas source aligns with the quadrotor position. The second design is a half-open space where the obstacle is placed in front of the gas source, but there is a gap for the gas flows directly toward the palm-sized quadrotor. Therefore, developing a GSL robot using a palm-sized quadrotor should satisfy the aim, which is the payload limit, and time limit using two design cases. The gas sensor position validation is done using PIV, and in this study, the searching focus is limited to the 2D area.

2.2. Command execution system and power

The role of the CES is critical to determining the behavior of a palm-sized quadrotor. The CES consists of the Arduino block from Sparkfun and Intel Edison as the control board. Each CES component communicates and transmits the data from the sensors and decides the behavior for palm-sized quadrotor movements. For detail, please see Figure 1. The CES collects the data from the sensor by using Arduino and transfers it to the server through Intel Edison as the core part handles the data transfer via Wi-Fi communication. All processes to execute the command behavior are conducted automatically without human intervention, except the initial palm-sized quadrotor take-off, landing, turn-on, and turn-of-the-system power. Inside the CES, communication between Arduino and Intel Edison to pass the data uses serial and I2C communication depending on the type of sensor attached to the CES.
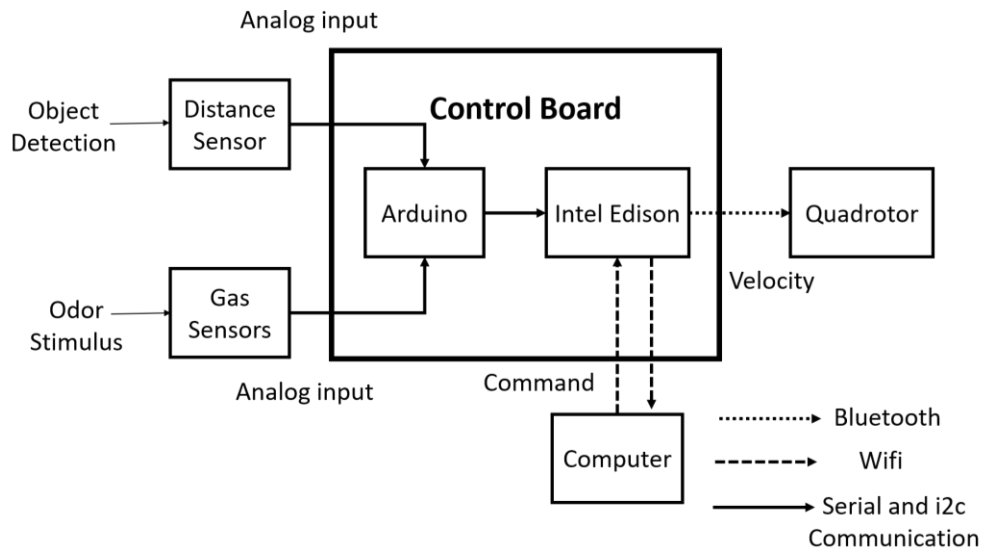
Figure 1. Diagram block of command center

Another important part to support the CES is the power system battery. The battery to support both CES and palm-sized quadrotors is selected carefully. The quadrotor's battery uses the Morpillot Li-Po battery (Amazon.jp) with a 3.7 V 600 mAh and a weight of 9.07 g. CES's power is used Li-Po battery 3.7 V 380 mAh, with a weight approximation of 10.3 g. The battery's power systems are separated to minimize the complexity of merging the different voltage consumption between a palm-sized quadrotor and CES. Typically, the flight drains more power instead of supporting the hardware system.

2.3. Sensors selection and configuration

In this study, the primary sensors are gas and distance sensors. Since the palm-sized quadrotor has a size limitation, however, a small size sensor is selected. Here, the gas sensor uses MEMs MiCS-5524 Gas Sensor Breakout (Adafruit), which has small dimensions of $20.0 \times 12.7 \times 3.1$ mm with a weight of 0.9 g, the MiCS-5524 sensor has a performance almost equal to the natural silkmoth antennae [37].

To support the palm-sized quadrotor avoids any obstacle, a MEMS size VL53L0X is chosen where it has a dimension $21.0 \times 18.0 \times 2.8$ mm with 1.3 g of the weight. The sensor also can detect the object from two meters away. Two meters range of detection can give time to a palm-size quadrotor to decide if the computational speed is low. Hence, both gas and distance sensors satisfy the criterion of small size and lightweight. Then, the gas sensor position needs validation, where the validation performs by conducting a PIV to study the wind flow's chemical distribution [38]. The analysis procedure is that the experiment should be conducted in a room without light or completely dark. The analysis uses a laser, and this condition aims to obtain a satisfactory result to clearly understand the gas distribution behavior, as illustrated in Figure 2.

The PIV study suggests that the sensor position is located in the front of a palm-sized quadrotor. Thus, the gas sensor's position is ideally mounted on the front of the quadrotor body, assuming the gas distribution approach from the front side. However, including Intel Edison (5.2 g) and Arduino block from Sparkfun (7.5 g), the total load is 38 gr which means, this result achieves less than the allowed weight of 40 gr. The list of components is shown in Table 1.
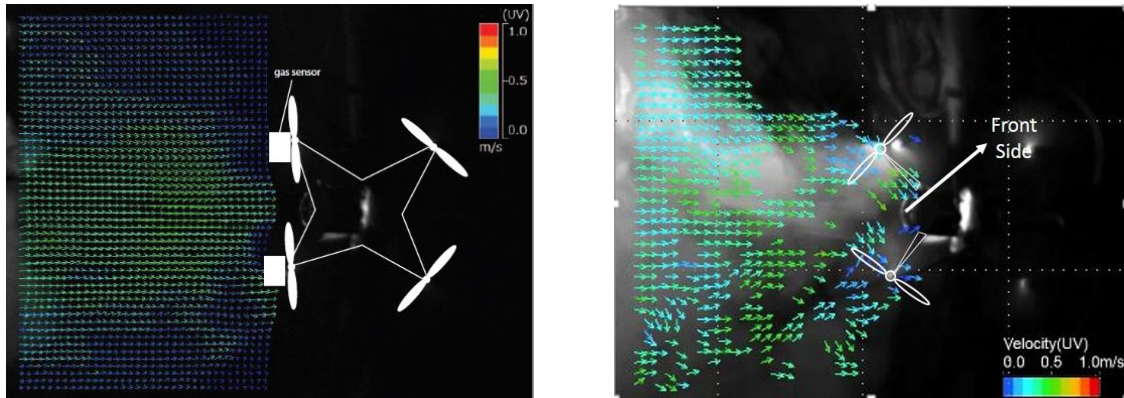
Figure 2. Condition of gas distribution in same flow with the condition before and after affected by the rotation of palm-sized quadrotor propellers

Table 1. Component detail

	Name
Processing Unit	Intel Edison
	Arduino block from Sparkfun
Gas sensors	MiCS-5524
Distance Sensor	VL53L0X
Palm-sized quadrotor	parrot mini-drone mambo FPV (Parrot Inc),

2.4. Palm-sized quadrotor searching mechanism
2.4.1. Palm-sized quadrotor dynamics
Consider a palm-sized quadrotor flight in two dimensions space x-y plane with z-axis is fixed. The dynamic of the quadrotor in two dimensions is given by (1):

$$\dot{q} = f(q, u) \tag{1}$$

where $q = [x \quad y \quad \psi]^T$ and $u = [u_x \quad u_y \quad u_\psi]^T$ are the global position and local input control, respectively. As the q holds the global terms for the position, then the dynamics can be described in (2):

$$\begin{bmatrix} \dot{x} \\ \dot{y} \\ \dot{\psi} \end{bmatrix} = \begin{bmatrix} \cos\psi & -\sin\psi & 0 \\ \sin\psi & \cos\psi & 0 \\ 0 & 0 & 1 \end{bmatrix} \begin{bmatrix} u_x \\ u_y \\ u_\psi \end{bmatrix} \tag{2}$$

Thus, the quadrotor model in (2) defines by (3):

$$\begin{aligned} \dot{x} &= u_x \cos\psi - u_y \sin\psi, \\ \dot{y} &= u_x \sin\psi + u_y \cos\psi, \\ \dot{\psi} &= u_\psi. \end{aligned} \tag{3}$$

2.4.2. Sensor data pre-processing and searching mechanism
The searching mechanism starts by obtaining data from the gas sensor and determining the action which satisfies the threshold after several data pre-processing. Now, assuming the sensor detection is sequential, then, $s \in [s_l, s_r]$ is the data from the gas sensor for the left and right sides, respectively. The gas detection has the potential that the noise disturbs the data reading. In order to reduce the noise, average means filter (AM) is employed, which define by (4):

$$\bar{s}(k) = \frac{1}{n} \sum_{i=1}^{N} s(k - i) \tag{4}$$

where, $\bar{s}(k)$ is the output data sensor after filtering, and $s(k - i)$ is the raw data sensor before noise reduction. However, the after-filtering data may give a true false detection. Then, the inverse model based on autoregressive exogenous (ARX) to estimate true input is introduced to avoid the false detection. This model

will simplify the determination of behavior patterns for the palm-sized quadrotor. The implementation of the ARX model to estimate the ethanol gas detection to both the left and the right gas sensors defines by (5):

$$\hat{s}(k) = b_0 s(k) + b_1 s(k-1) - a_1 \hat{s}(k-1) - a_2 \hat{s}(k-2). \tag{5}$$

The parameter of a_1, a_2, b_0, b_1 are the coefficient of estimation determines by linear least squares. The in (5) is applied to both left and right gas sensors. Thus, $\hat{s} \in [\hat{s}_l, \hat{s}_r]$ is the estimation calculation for the gas sensor on the left and right sides. The calculation in (5) is compared with the gas sensor threshold δ to obtain the logical result. We denote the logical result $m \in [0,1]$ by checking the value of $\hat{s}$ define by (6):

$$m = \begin{cases} 1, & \hat{s}(k) \le \delta \\ 0, & \hat{s}(k) \ge \delta \end{cases} \tag{6}$$

Then, the comparison between two sensors is needed to determine the quadrotor turning direction, which is set for each $\hat{s}_l$ and $\hat{s}_r$. The turning direction is elucidated in algorithm 1. The time t is set by 5 seconds.

Algorithm 1. Algorithm of silkmoth pseudocode

```
1:     Input Gas Input stimuli, s ≠ 0
2:     Output Behavioral movement
3:     Do calculation in equation (2) and (3)
4:     If ŝ_l ≤ δ or ŝ_r ≤ δ then
5:             Perform surge
6:             If ŝ_l < ŝ_r then
7:                     Do zigzag motion, turning to left
8:                     Do time counting, t++
9:                     If t == 5 then
10:                            Do a loop motion, turning direction to the left side
11:                    endif
12:            endif
13:            If ŝ_r < ŝ_l then
14:                    Do zigzag motion, turning to left
15:                    Do time counting, t++
16:                    If t == 5 then
17:                            Do a loop motion, turning direction to the right side
18:                    endif
19:            endif
20:    Endif
```

2.4.3. Palm-sized quadrotor surge motion

The silkmoth mechanism starts when $\hat{s}(k) \le \delta$. The behavior of the silkworm is embedded into the sequential motion shown in Figure 3. Figure 3 shows the behaviors of silkmoth correspond to Algorithm 1.
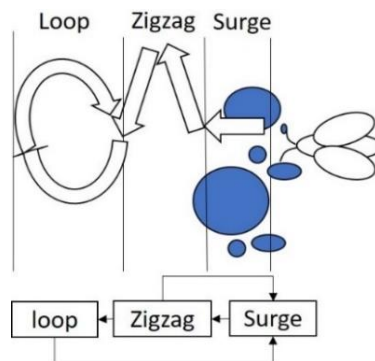

Figure 3. Silkmoth mechanism

The surge event occurs when the gas detection satisfies the (6). Thus, the palm-sized quadrotor will perform a surge with the surge speed is defined by (7);

$$surge = K_s m \tag{7}$$

where, K_s is the desired gain for a surge. This surge parameter will influence the speed of the quadrotor when it detects the gas. When the sensors are not detecting any odor cues. Then, the palm-sized quadrotor will continue to the following behavioral state to zigzag and looping.

2.4.4. Palm-sized quadrotor zigzag and loop motion

Determining the turning direction for zigzag and looping can be extracted from the information of the first sensor that detects the gas. For example, when the left sensor detects the gas, the turning direction after surge will change to zigzag, turning directly to the left side. As for the right-side sensor to detect the information, the turning direction will turn to the right side. A random turning direction if each sensor detects the gas substance simultaneously. The turning duration for zigzag is 5 seconds. Suppose the sensor lost the gas information while in the middle of the zigzag state, the behavioral motion will change to looping when the times already passed from 5 seconds. The $t = 5$ corresponds to the algorithm in Algorithm 1.

2.4.5. Obstacle avoidance

Obstacle avoidance is designed to ensure the safety of the palm-sized quadrotor when searching in an environment with an obstacle. The three distance sensors are attached following this configuration (front, left, and right) side of the quadrotor. To activate the quadrotor behaviors when the distance sensors detect any obstacle in their position. Let set the threshold η as the reference for the minimum distance to prevent the collision. The behavior of the quadrotor to prevent the collision is then described by (8);

$$p = \begin{cases} 1, & d(k) \leq \eta \\ 0, & d(k) \geq \eta \end{cases} \tag{8}$$

where, p is the logical operator, where $p \in [0,1]$. The parameter of $d(k)$ is the distance sensor parameter. Then, the speed to avoid collision with the object is defined by (9).

$$avoid = -k_o p \tag{9}$$

In (9), K_o is the desired gain of avoidance. Therefore, in (9) can be applied in the x-y plane. The negative sign means the effort of the quadrotor to escape from the collision. There will be two turning states when the palm-sized quadrotor starts searching based on the flowchart in Figure 4. The first is when it detects the gas information, and the second is when it detects the obstacle. When the palm-sized quadrotor approaches the obstacle, it will switch its behavior to obstacle avoidance. The switching behavior changes depending on which information the systems receive.
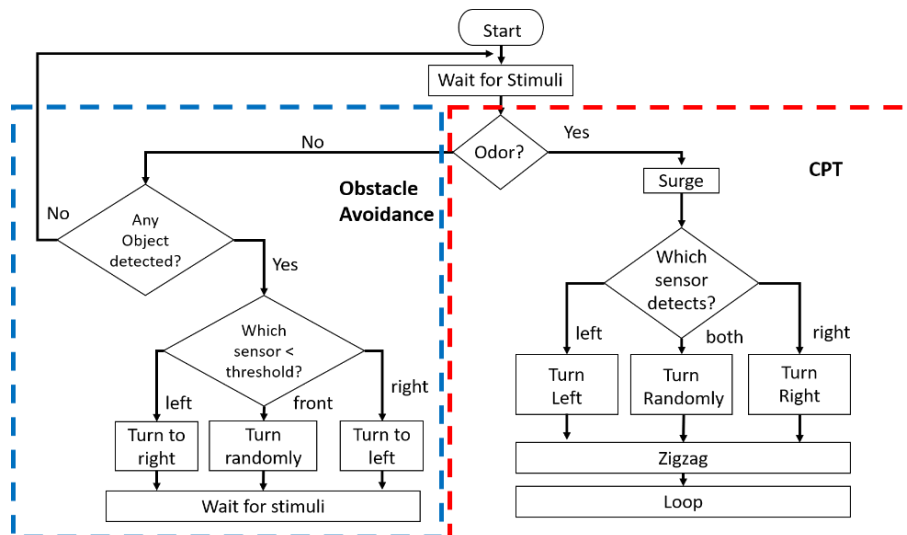

Figure 4. Flowchart of GSL and obstacle avoidance in palm-sized quadrotor

To add the obstacle avoidance technique, in the x-y axis should be stated where the proposed a repulsion-force based to improve the quadrotor capability which defines by (10).

$$
\begin{aligned}
u_x &= avoid_{net}, \\
&= -K_0 p_{net}, \\
&= -K_0 p_l - K_0 p_r.
\end{aligned} \tag{10}
$$

where p_l and p_r represent the sensor on the palm-sized quadrotor's left and right-side logical operator, which has the same function as (9). Next, the input control in the y-axis is affected by one distance sensor and gas sensor to decide the GSL motion as surge. Thus, the u_y will be (11),

$$
\begin{aligned}
u_y &= surge + avoid_{net}, \\
&= K_s m - K_0 p_{net}, \\
&= K_s m - K_0 p_f
\end{aligned} \tag{11}
$$

where p_f is representing the logical operator of the distance sensor on the front side. For $u_\psi = f(t)$ where $f(t)$ is piecewise continuous function. Therefore, the configuration of the quadrotor model will be (12),

$$
\begin{bmatrix} \dot{x} \\ \dot{y} \\ \dot{\psi} \end{bmatrix} = \begin{bmatrix} \cos\psi & -\sin\psi & 0 \\ \sin\psi & \cos\psi & 0 \\ 0 & 0 & 1 \end{bmatrix} \begin{bmatrix} -K_0 p_l - K_0 p_r \\ K_s m - K_0 p_f \\ f(t) \end{bmatrix} \tag{12}
$$

2.5. Experimental design

In this study, the performance of GSL is validated in an obstacle environment. Therefore, two scenarios will be offered to validate the search performance: the first scenario is the obstacle in front of the gas source. The second scenario is that the obstacle is in the front of the source, but there is space to let the gas flow. The gas source's experimental design 1 and 2 is shown in Figures 5 (a) and 5(b).
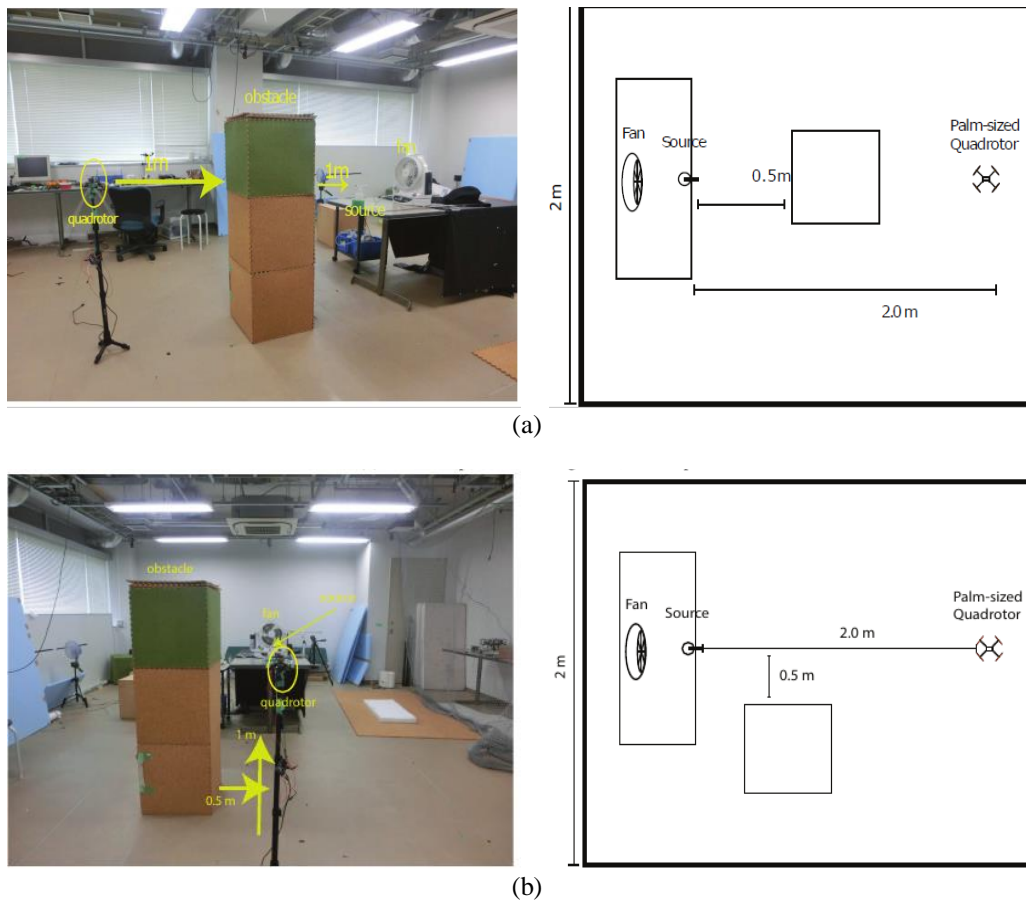

(a)

(b)

Figure 5. Experimental design: (a) obstacle blocks the source and (b) obstacle blocks the source with a certain gap

The experimental design is set to validate the GSL and the obstacle avoidance performance. In this experiment, the gas flows continuously and directly toward the quadrotor's location, the flow rate is 1L per min, the wind speed is 0.65 ms measured by an anemometer, and the palm-sized quadrotor's height level is 1m. The room temperature is set to $24\,°C$ and the humidity level is 40%. After each trial, the exhaust fan is turned on to keep the environment less from ethanol pollutants, disturbing the sensor reading. Moreover, the quadrotor speed is set at 5 cm/s. The coefficient of ARX is set -0.981, 0.01653, 0.2833, -0.2706 for a_1, a_2, b_0, b_1, respectively. The threshold for gas detection is set at 0.033 for each left sensor and the right sensor. The duration of searching maximum is 80 seconds considering the palm-sized quadrotor time duration because of carrying the payload.

3. RESULT AND DISCUSSION

In the experiment, the quadrotor conducts the GSL in two environmental designs. Before elucidating the GSL performance, the total payload for GSL system design is achieved at a weight of 38 gr lower than the allowed payload weight of 40 gr, where the limit of 40 gr is the threshold for maximum take-off weight excludes the frame and the internal battery. The parameters elucidated in the experimental design section, the quadrotor runs using node.js programming language. The programming language is chosen because node.js provides a library to control the parrot mini-drone and the sensor straightforwardly. The first trial is conducting the GSL in the environmental design shown in Figure 5(a) to test the system's effectiveness. The result and trajectory obtained in this experiment based on Figure 5(a) configuration are shown in Figure 6, where searching performance is shown in Table 2.

It is interesting to know that searching in blocked space, the success rate is 0%. Further investigation, a significant problem is faced in our platform: the compatibility of a searching algorithm that must compensate for the time limit during the mission. The palm-sized quadrotor's incompatibility can be caused by the gas source concentration dispersed to the position of the palm-sized quadrotor itself is weak. This result is thanks to the obstacle that blocks the source. This result confirms the experiment conducted in [39], which shows that the visualization of the gas flow reduces significantly. Another research that confirms the challenge of searching in the environment in Figure 6 was mentioned in [40]. In [40] result, it is known in the backside of the obstacle that the gas concentration is low thanks to the near-wake region. Therefore, the palm-sized quadrotor only repeated the surge-zigzag-loop pattern in this experiment until it depleted its battery.
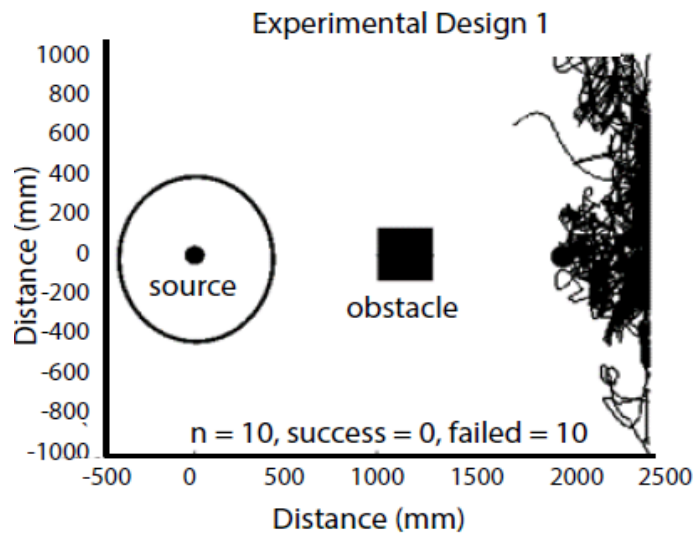

Figure 6. Result in experimental design follows Figure 5(a)

Table 2. GSL Performance with experimental design in Figure 5(a)

	Success	Unsuccess
Trials	0	10
Average searching time	0s	>80 s
Minimum searching time	0s	>80 s
Maximum searching time	0s	>80 s

On the other hand, the wind contributes to creating a wake around the obstacle. The wake phenomenon that occurs around the obstacle caused the gas substance to flock near the obstacle. As the gas substance flock in the rear part of the obstacle, the concentration increases not in the part of the obstacle headed to the palm-sized quadrotor. The investigation of gas searching continues to experimental design 2. The success rate in searching the gas source is 80% see Table 3 and Figure 7. Here, the success rate is significantly different from the experimental design 1. This success searching result (design in Figure 5(b) if we compare with [1] is increased wherein the previous research [1] approximately: 70% of success rate this thanks to the flow of the gas which its direction affected by the position of the obstacle. The searching success rate is also contributed by a gas distribution which is not diluted because of blocked by an obstacle. This result also confirms [40] result. To validate the GSL, we conduct experimentation in two experimental designs. This result confirms that the obstacle position design directly affects the unimpeded gas substance flow to the palm-sized quadrotor. The exciting part of experimental design 2 in Figure 5(b) is that the unsuccessful attempt occurred because the systems hardly recognize the gas information, which causes the searching time to exceed the limit. The algorithm of potential function to avoid the collision is successfully managed by the palm-sized quadrotor to avoid the crash.

Table 3. GSL performance with experimental design in Figure 5(b)

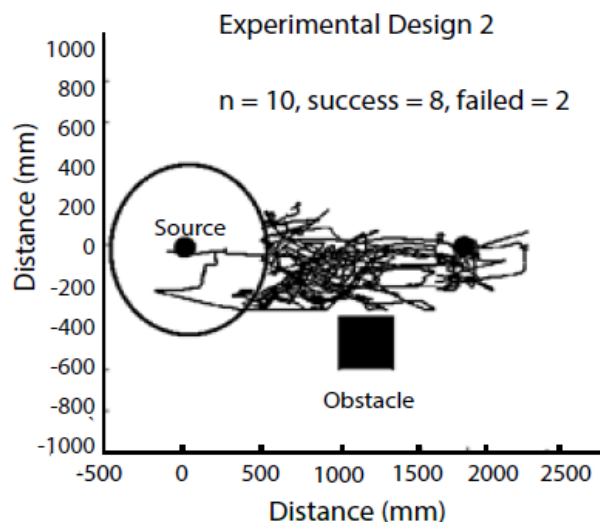|	Success	Unsuccess
Trials	8	2
Average Searching time	31.4 s	81.25 s
Minimum searching time	15 s	30 s
Maximum searching time	70 s	120 s

Figure 7. GSL performance with design in Figure 5(b)

4. CONCLUSION

This paper demonstrates a GSL using a palm-sized quadrotor in the obstacle environment and verified through experimental validation. This paper has developed a 38-gr system of the palm-sized quadrotor, consisting of obstacle avoidance and GSL systems and below the allowed payload limitation. The performance of searching in the obstacle region varies in two designs where it achieves 0% and 80% with the explanation in the previous section. Based on the results, the algorithm of the insect behavior works appropriately to respond to the gas information. This result confirms that the GSL algorithm can work simultaneously with obstacle avoidance. This result also proves the GSL integration with obstacle avoidance (modified bio-inspired). According to the palm-sized quadrotor conditions, improving gas detection design and algorithm is required. Moreover, the limited payload size also needs consideration because the quadrotor design is relatively small.

This study considers the drawbacks that occurred in Figure 6. The gas distribution is significantly reduced in configuration Figure 5(a). The bio-inspired algorithm employed in this study works if there is a gas detection. However, when the gas information is lost due to a particular condition, such as an obstacle. In

that case, the recommendation for future reference is that the system must be improved by adding an active searching algorithm or using a palm-sized quadrotor with a built-in visual system to improve navigation. Searching in 3D also can be considered to validate the performance of the proposed algorithm.

REFERENCES

[1] M. R. Fikri, "Gas source localization using bio-inspired algorithm for mini flying sniffer robot : development and experimental investigation," *Computer Engineering and Applications*, vol. 9, no. 3. pp. 207–214, 2020, doi: 10.18495/COMENGAPP.V9I3.343.

[2] S. Shigaki, M. Fikri, and D. Kurabayashi, "Design and experimental evaluation of an odor sensing method for a pocket-sized quadcopter," *Sensors*, vol. 18, no. 11, Nov. 2018, doi: 10.3390/s18113720.

[3] P. P. Neumann, V. Hernandez Bennetts, A. J. Lilienthal, M. Bartholmai, and J. H. Schiller, "Gas source localization with a micro-drone using bio-inspired and particle filter-based algorithms," *Advanced Robotics*, vol. 27, no. 9, pp. 725–738, Jun. 2013, doi: 10.1080/01691864.2013.779052.

[4] J. Burgués, V. Hernández, A. Lilienthal, and S. Marco, "Smelling nano aerial vehicle for gas source localization and mapping," *Sensors*, vol. 19, no. 3, Jan. 2019, doi: 10.3390/s19030478.

[5] K. S. Eu and K. M. Yap, "Chemical plume tracing," *International Journal of Advanced Robotic Systems*, vol. 15, no. 1, Jan. 2018, doi: 10.1177/1729881418755877.

[6] A. H. Reddy, B. Kalyan, and C. S. N. Murthy, "Mine rescue robot system – a review," *Procedia Earth and Planetary Science*, vol. 11, pp. 457–462, 2015, doi: 10.1016/j.proeps.2015.06.045.

[7] D. Hollenbeck, M. Dahabra, L. E. Christensen, and Y. Chen, "Data quality aware flight mission design for fugitive methane Sniffing using fixed wing sUAS," *2019 International Conference on Unmanned Aircraft Systems (ICUAS)*, vol. 1, pp. 813–818, Jun. 2019, doi: 10.1109/ICUAS.2019.8798176.

[8] L. Golston *et al.*, "Natural gas fugitive leak detection using an unmanned aerial vehicle: localization and quantification of emission rate," *Atmosphere*, vol. 9, no. 9, Aug. 2018, doi: 10.3390/atmos9090333.

[9] J. Palacín *et al.*, "Application of an array of metal-oxide semiconductor gas sensors in an assistant personal robot for early gas leak detection," *Sensors*, vol. 19, no. 9, pp. 1–16, Apr. 2019, doi: 10.3390/s19091957.

[10] W. Krüll, R. Tobera, I. Willms, H. Essen, and N. von Wahl, "Early forest fire detection and verification using optical smoke, gas and microwave sensors," *Procedia Engineering*, vol. 45, pp. 584–594, 2012, doi: 10.1016/j.proeng.2012.08.208.

[11] C. Yuan, Y. Zhang, and Z. Liu, "A survey on technologies for automatic forest fire monitoring, detection, and fighting using unmanned aerial vehicles and remote sensing techniques," *Canadian Journal of Forest Research*, vol. 45, no. 7, pp. 783–792, Jul. 2015, doi: 10.1139/cjfr-2014-0347.

[12] J. Roldán, G. Joossen, D. Sanz, J. del Cerro, and A. Barrientos, "Mini-UAV based sensory system for measuring environmental variables in greenhouses," *Sensors*, vol. 15, no. 2, pp. 3334–3350, Feb. 2015, doi: 10.3390/s150203334.

[13] J. Valente, R. Almeida, and L. Kooistra, "A comprehensive study of the potential application of flying ethylene-sensitive sensors for ripeness detection in apple orchards," *Sensors*, vol. 19, no. 2, Jan. 2019, doi: 10.3390/s19020372.

[14] J. Burgués and S. Marco, "Environmental chemical sensing using small drones: a review," *Science of The Total Environment*, vol. 748, Dec. 2020, doi: 10.1016/j.scitotenv.2020.141172.

[15] R. Bilger, "Turbulent diffusion flames," *Annual Review of Fluid Mechanics*, vol. 21, no. 1, pp. 101–135, Jan. 1989, doi: 10.1146/annurev.fluid.21.1.101.

[16] S. Edwards, A. J. Rutkowski, R. D. Quinn, and M. A. Willis, "Moth-inspired plume tracking strategies in three-dimensions," in *Proceedings of the 2005 IEEE International Conference on Robotics and Automation*, 2005, vol. 2005, pp. 1669–1674, doi: 10.1109/ROBOT.2005.1570353.

[17] F. van Breugel and M. H. Dickinson, "Plume-tracking behavior of flying drosophila emerges from a set of distinct sensory-motor reflexes," *Current Biology*, vol. 24, no. 3, pp. 274–286, Feb. 2014, doi: 10.1016/j.cub.2013.12.023.

[18] A. Liu, A. E. Papale, J. Hengenius, K. Patel, B. Ermentrout, and N. N. Urban, "Mouse navigation strategies for odor source localization," *Frontiers in Neuroscience*, vol. 14, pp. 1–16, Mar. 2020, doi: 10.3389/fnins.2020.00218.

[19] F. Rahbar, A. Marjovi, P. Kibleur, and A. Martinoli, "A 3-D bio-inspired odor source localization and its validation in realistic environmental conditions," *2017 IEEE/RSJ International Conference on Intelligent Robots and Systems (IROS)*, vol. 2017, pp. 3983–3989, Sep. 2017, doi: 10.1109/IROS.2017.8206252.

[20] N. A. Syafinaz, D. Pebrianti, L. Bayuaji, R. Hamid, and N. Qasrina Ann, "Swarm robotics target searching strategy based on extended bat algorithm," *Indonesian Journal of Computing, Engineering and Design (IJoCED)*, vol. 2, no. 2, Oct. 2020, doi: 10.35806/ijoced.v2i2.113.

[21] A. Liberzon, K. Harrington, N. Daniel, R. Gurka, A. Harari, and G. Zilman, "Moth-inspired navigation algorithm in a turbulent odor plume from a pulsating source," *PLOS ONE*, vol. 13, no. 6, Jun. 2018, doi: 10.1371/journal.pone.0198422.

[22] G. C. H. E. de Croon, L. M. O'Connor, C. Nicol, and D. Izzo, "Evolutionary robotics approach to odor source localization," *Neurocomputing*, vol. 121, pp. 481–497, Dec. 2013, doi: 10.1016/j.neucom.2013.05.028.

[23] S. Shigaki *et al.*, "Animal-in-the-loop system to investigate adaptive behavior," *Advanced Robotics*, vol. 32, no. 17, pp. 945–953, Sep. 2018, doi: 10.1080/01691864.2018.1511473.

[24] C. Ercolani and A. Martinoli, "3D odor source localization using a micro aerial vehicle: system design and performance evaluation," *2020 IEEE/RSJ International Conference on Intelligent Robots and Systems (IROS)*, pp. 6194–6200, Oct. 2020, doi: 10.1109/IROS45743.2020.9341501.

[25] K. S. Eu, K. M. Yap, and T. H. Tee, "An airflow analysis study of quadrotor based flying sniffer robot," *Applied Mechanics and Materials*, vol. 627, pp. 246–250, Sep. 2014, doi: 10.4028/www.scientific.net/AMM.627.246.

[26] M. Hutchinson, C. Liu, and W. Chen, "Source term estimation of a hazardous airborne release using an unmanned aerial vehicle," *Journal of Field Robotics*, vol. 36, no. 4, pp. 797–817, Jun. 2019, doi: 10.1002/rob.21844.

[27] J. Monroy, J.-R. Ruiz-Sarmiento, F.-A. Moreno, F. Melendez-Fernandez, C. Galindo, and J. Gonzalez-Jimenez, "A semantic-

based gas source localization with a mobile robot combining vision and chemical sensing," *Sensors*, vol. 18, no. 12, Nov. 2018, doi: 10.3390/s18124174.

[28] H. Ishida, H. Tanaka, H. Taniguchi, and T. Moriizumi, "Mobile robot navigation using vision and olfaction to search for a gas/odor source," *Autonomous Robots*, vol. 20, no. 3, pp. 231–238, Jun. 2006, doi: 10.1007/s10514-006-7100-5.

[29] A. Gongora, J. Monroy, and J. Gonzalez-Jimenez, "Gas source localization strategies for teleoperated mobile robots. An experimental analysis," *2017 European Conference on Mobile Robots (ECMR)*. IEEE, pp. 1–6, Sep. 2017, doi: 10.1109/ECMR.2017.8098720.

[30] A. Loutfi, S. Coradeschi, L. Karlsson, and M. Broxvall, "Putting olfaction into action: using an electronic nose on a multi-sensing mobile robot," in *2004 IEEE/RSJ International Conference on Intelligent Robots and Systems (IROS) (IEEE Cat. No.04CH37566)*, 2004, vol. 1, pp. 337–342, doi: 10.1109/IROS.2004.1389374.

[31] A. Marjovi and L. Marques, "Multi-robot odor distribution mapping in realistic time-variant conditions," *2014 IEEE International Conference on Robotics and Automation (ICRA)*. IEEE, pp. 3720–3727, May 2014, doi: 10.1109/ICRA.2014.6907398.

[32] J. G. Monroy, J.-L. Blanco, and J. Gonzalez-Jimenez, "Time-variant gas distribution mapping with obstacle information," *Autonomous Robots*, vol. 40, no. 1, pp. 1–16, Jan. 2016, doi: 10.1007/s10514-015-9437-0.

[33] T. Takasaki, S. Namiki, and R. Kanzaki, "Use of bilateral information to determine the walking direction during orientation to a pheromone source in the silkmoth Bombyx mori," *Journal of Comparative Physiology A*, vol. 198, no. 4, pp. 295–307, Apr. 2012, doi: 10.1007/s00359-011-0708-8.

[34] R. A. Russell, A. Bab-Hadiashar, R. L. Shepherd, and G. G. Wallace, "A comparison of reactive robot chemotaxis algorithms," *Robotics and Autonomous Systems*, vol. 45, no. 2, pp. 83–97, Nov. 2003, doi: 10.1016/S0921-8890(03)00120-9.

[35] G. Kowadlo and R. A. Russell, "Robot odor localization: a taxonomy and survey," *The International Journal of Robotics Research*, vol. 27, no. 8, pp. 869–894, Aug. 2008, doi: 10.1177/0278364908095118.

[36] P. G. Fahlstrom and T. J. Gleason, "Introduction to UAV Systems." John Wiley & Sons, Ltd, Chichester, UK, Aug. 2012, doi: 10.1002/9781118396780.

[37] S. Shigaki, K. Okajima, K. Sanada, and D. Kurabayashi, "Experimental analysis of the influence of olfactory property on chemical plume tracing performance," *IEEE Robotics and Automation Letters*, vol. 4, no. 3, pp. 2847–2853, Jul. 2019, doi: 10.1109/LRA.2019.2921948.

[38] R. J. Adrian, "Twenty years of particle image velocimetry," *Experiments in Fluids*, vol. 39, no. 2, pp. 159–169, Aug. 2005, doi: 10.1007/s00348-005-0991-7.

[39] I. Mavroidis, R. F. Griffiths, and D. J. Hall, "Field and wind tunnel investigations of plume dispersion around single surface obstacles," *Atmospheric Environment*, vol. 37, no. 21, pp. 2903–2918, Jul. 2003, doi: 10.1016/S1352-2310(03)00300-5.

[40] I. Mavroidis, S. Andronopoulos, J. G. Bartzis, and R. F. Griffiths, "Atmospheric dispersion in the presence of a three-dimensional cubical obstacle: Modelling of mean concentration and concentration fluctuations," *Atmospheric Environment*, vol. 41, no. 13, pp. 2740–2756, Apr. 2007, doi: 10.1016/j.atmosenv.2006.11.051.

BIOGRAPHIES OF AUTHORS

Muhamad Rausyan Fikri is an Information Systems lecturer at Sampoerna University. He received his Bachelor of Science (B.Sc.) at Universitas Gadjah Mada, Department of Computer Science and Electronics in 2015 and Master of Engineering (M.Eng.) at Tokyo Institute of Technology, Department of Systems and Control Engineering in 2018. His research interests include bioinspired robot, cooperative control, and IoT. He is currently also the Coordinator of IoT Lab and Cyber-Physical Research group at Sampoerna University Email: muhamad.fikri@sampoernauniversity.ac.id.

Djati Wibowo Djamari received B.Eng., M.Eng., and Ph.D. degrees in Mechanical Engineering from Institut Teknologi Bandung (ITB) in 2007, Nanyang Technological University (NTU) in 2010, and National University of Singapore in 2020, respectively. From 2009 to 2013 he had a position as Research Associate at School of Mechanical and Aerospace Engineering of NTU and from 2013 to 2014 he was an Academic Assistant at the Mechanical Engineering study program of ITB. He is currently a Lecturer in Mechanical Engineering study program of Sampoerna University, Jakarta, Indonesia. His research interests include distributed control of multi-agent systems, vibration control and vehicle dynamics and control. Email: djati.wibowo@sampoernauniversity.ac.id.